



Open Research Online

The Open University's repository of research publications and other research outputs

Characterization of mesostasis areas in mare basalts: constraining melt compositions from which apatite crystallizes

Conference or Workshop Item

How to cite:

Potts, N. J.; Tartèse, R.; Anand, M.; Franchi, I. A.; van Westrenen, W.; Barnes, Jessica and Griffiths, A. A. (2014). Characterization of mesostasis areas in mare basalts: constraining melt compositions from which apatite crystallizes. In: 45th Lunar and Planetary Science Conference, 17-21 Mar 2014, Houston, Texas.

For guidance on citations see [FAQs](#).

© 2014 The Author

Version: Version of Record

Copyright and Moral Rights for the articles on this site are retained by the individual authors and/or other copyright owners. For more information on Open Research Online's data [policy](#) on reuse of materials please consult the policies page.

oro.open.ac.uk

CHARACTERIZATION OF MESOSTASIS AREAS IN MARE BASALTS: CONSTRAINING MELT COMPOSITIONS FROM WHICH APATITE CRYSTALLIZES. N. J. Potts^{1,2*}, R. Tartèse¹, M. Anand^{1,3}, I. A. Franchi¹, W. van Westrenen², J. J. Barnes^{1,3}, A. A. Griffiths^{1,4} ¹Department of Physical Sciences, The Open University, Milton Keynes, UK, (*nicola.potts@open.ac.uk) ²Faculty of Earth and Life Sciences, VU University Amsterdam, NL ³Department of Earth Sciences, The Natural History Museum, London, UK. ⁴School of Earth, Atmospheric and Environmental Science, University of Manchester, UK.

Introduction: Crystallization of major silicate and oxide phases from basaltic melts produces late-stage liquids whose chemical compositions differ from the initial melt. These chemically evolved liquids crystallize phases in the interstitial mesostasis regions in lunar basaltic rocks. Enrichment of incompatible elements, including volatiles such as OH, F, Cl, is characteristic of these late-stage liquids and encourages growth of accessory phases including apatite [$\text{Ca}_5(\text{PO}_4)_2(\text{F},\text{Cl},\text{OH})$]. Apatite is the main volatile bearing crystalline phase in lunar rocks. It starts crystallizing after ~ 95 % melt solidification in typical mare basalts [1], but could crystallize earlier, after ~ 85 - 90 % solidification in KREEP basalts. Using the OH contents of apatites, several researchers have calculated water contents for parental magmas. These calculated parental magma water contents can then be used to estimate a range of values for water in the mantle source regions of mare basalts [e.g., 2 - 6]. Therefore, a better characterization of the mesostasis areas, and of the melts in which apatite forms, is paramount to gain further insights and constraints on water in the lunar interior, especially because important parameters such as partitioning of volatiles between late-stage melts and apatite remain poorly constrained.

In this study, we have focused on the analysis of mesostasis regions from four Apollo mare basalts (10044, 12064, 15058, and 70035). These analyses are compared to data on mesostasis regions of two lunar basaltic meteorites (MIL 05035; LAP 02205) [7 - 9] to gain insight into inter-sample variability. We also report results from apatite solubility modelling [10, 11] and modelling of crystallization of different basaltic melts performed using the MELTS [12] and SPICES [13] software. The aim is to provide an accurate composition for bulk melt from which apatite is expected to crystallize. MELTS is a rigorous thermodynamic model of crystal-liquid equilibria calibrated from experimentally derived data for specific compositional dependences, temperature, pressure and $f\text{O}_2$. SPICES is a recently developed program utilizing previous models of lunar magma fractional and equilibrium crystallization [13].

Samples and Methods: The samples from this study are all mare basalts, and their mineralogy and petrology are reported in a companion abstract [14]. Each sample contains multiple regions of mesostasis.

For this study, only those mesostasis regions with a wide variety of representative phases were chosen.

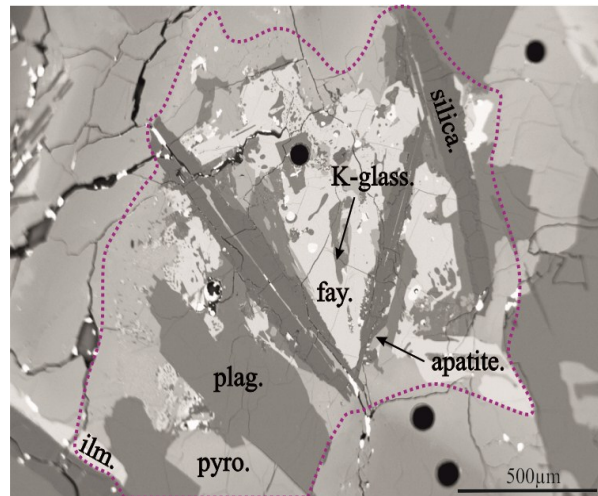


Figure 1: BSE image of a mesostasis region in 12064 (the thin dashed curve outlines the extent of the mesostasis). The main phases in the region are plagioclase (plg.), ilmenite (ilm.), pyroxene (pyro.), silica, fayalite (fay.), apatite and K-feldspar glass.

Quantitative phase analysis was carried out using the Cameca SX 100 electron microprobe at the Open University. An accelerating voltage of 20 kV, nominal probe current of 20 nA and a beam size of 1 - 10 μm were used. Apatite data were taken from [4]. Modal mineral and quench glass abundances were calculated using the ImageJ[®] software.

Modelling Methods: Bulk compositions serving as input for MELTS models in this study were taken from [15] and fractionally crystallized at a $f\text{O}_2$ of IW -2, 1000 bars and using liquidus temperatures calculated by MELTS. The melt was crystallized until a mesostasis composition was obtained, confirmed by the phases present. Conditions of each SPICES run were kept similar to those used in the MELTS application to compare and contrast the viability of each model for lunar applications.

Results: Mesostasis phases crystallize between pre-existing grains. EPMA transects across mesostasis boundaries show distinct compositional differences in feldspar SiO_2 and Al_2O_3 contents between grains firmly in and out of regions (Fig. 1). Furthermore, a gradual transition between these two end-member composi-

tions indicates diffusion into these grains from the mesostasis melt. This creates added complexity in confirming the already subjective boundaries of mesostasis regions. Similar compositional differences for SiO₂, MgO, and FeO content in pyroxenes in and out of mesostasis regions were also observed.

	10044	12064	15058	70035
SiO ₂	78.27	67.86	66.38	68.76
TiO ₂	1.09	2.92	2.47	5.63
Al ₂ O ₃	9.43	6.01	12.14	9.78
FeO	4.94	11.11	8.54	7.01
MnO	0.07	0.12	0.07	0.09
MgO	0.30	0.30	0.49	1.32
CaO	5.59	7.30	5.94	5.79
Na ₂ O	0.66	0.21	0.42	0.75
K ₂ O	0.14	1.42	2.15	0.15
P ₂ O ₅	0.01	2.06	0.04	-
Total	100.51	99.31	99.44	99.30

Table 1: Bulk compositions of mesostasis regions in Apollo samples based on EPMA data and modal abundances for the most representative area in each sample. All values are in wt.%.

The bulk mesostasis compositions recalculated from modal abundances and mineral chemistry (Table 1), and results of MELTS and SPICEs modelling are generally in good agreement. Differences between Al₂O₃, TiO₂, FeO and P₂O₅ were found between the sample and modeling methods. The Al₂O₃ and FeO differences can be explained by varying amounts of plagioclase and fayalite in the natural samples, which the models assume to be main phases in the mesostasis areas. As this study was interested in areas where apatite forms there is a bias in the sample results which reflects higher P₂O₅ contents. TiO₂ results between all three methods (sample, MELTS, SPICEs) were varied with very little systematic trends between low-Ti basalts and high-Ti basalts. Final compositions were compared to lunar granite data [16].

Discussion: Lunar granites contain higher average Na₂O and K₂O compared to the re-calculated mesostasis bulk-composition in this study. The bulk compositions of Apollo sample and lunar granite melts however were comparable for other oxides, confirming that late-stage melts evolved from extensive crystallization of mare magmas are highly silicic and compositionally similar to lunar granites.

It has been shown that phosphate saturation is dependent on temperature and liquid composition [10, 11]. Mesostasis SiO₂ compositions taken from Apollo samples together with MELTS and SPICEs modeling were input into calculations from [10] and [11]. These show that for average P₂O₅ values measured from

Apollo samples [4] optimum values of 5 wt.% CaO and 72 wt.% SiO₂ are required to induce phosphate saturation. Reducing SiO₂ concentrations increases the amount of P₂O₅ required to reach phosphate saturation while increasing CaO decreases it.

MELTS is a program developed for terrestrial systems and was unable to fractionally crystallize down to mesostasis melt compositions without the presence of H₂O. For one sample (12064) up to 2 wt.% H₂O had to be added for the system to work. SPICEs, however, is specifically designed for lunar systems. Anhydrous bulk compositions were able to fractionate in this model, however, the fractionation here is relatively simple. It is therefore suggested that future melt modelling studies on lunar samples should be preferentially carried out in SPICEs to minimize uncertainties.

Further Work: The primary purpose for this investigation was to determine a natural lunar composition in which apatite would form. Previous investigations of apatite-melt partitioning have been performed using basaltic bulk-compositions [17-18]. As apatite is an accessory phase found in mesostasis regions it may be unrealistic to expect apatite to form from a basaltic composition, a conclusion supported by the results of this study. Average mesostasis composition taken from this work will be used as a starting composition for work on lunar apatite-melt volatile partitioning experiments.

Acknowledgements: We thank NASA CAPTEM for allocation of Apollo samples. This work was funded by an STFC Studentship awarded to NJP and research grant to MA (Grant no. ST/I001298/1).

References: [1] McCubbin F. M. et al. (2011) *GCA*, 75, 5073-5093 [2] Tartèse R. and Anand M. (2013) *EPSL*, 361, 480-486 [3] Barnes J. J. et al. (2013) *Chem. Geol.*, 337-338, 48-55 [4] Tartèse R. et al. (2013) *GCA*, 122, 58-74 [5] McCubbin F. M. et al. (2010), *Am. Min.*, 95, 1141-1150 [6] Boyce J. W. et al. (2010) *Nature*, 466, 466-486 [7] Joy K. H. et al. (2008) *GCA*, 72, 3822-3844 [8] Liu Y. et al. (2009) *Met. & Plant. Sci.*, 44, 261-284 [9] Anand M. et al. (2006) *GCA*, 70, 246 - 264 [10] Tollari N. et al. (2006) *GCA*, 70, 1518-1536 [11] Watson E.B. and Harrison T. (1984) *Phys. Earth & Plant. Inter.*, 35, 19-30 [12] Ghiorso M. S. et al. (2002) *G3*, 3(5), 1525-2027 [13] Davenport J. et al. (2013) *In Press with Comp. and Geosci. (Sept 2013)* [14] Griffiths A. A. et al. (2014) *LPSC XLIV (This meeting)* [15] Meyer C. (2011) *Lunar Sample Compendium* [16] Seddio S. et al. (2013) *Am. Mineral.*, 98, 1697-1713 [17] Prowatke S. and Klemme S. (2006) *GCA*, 70, 4513-4527. [18] Vander Kaaden K.E. et al. (2012) *LPSC XLIII*, Abstract #1247.